12^{th} International Conference on Fracture Mechanics of Concrete and Concrete Structures
FraMCoS-12
B.L.A. Pichler, Ch. Hellmich, P. Preinstorfer (Eds)

https://doi.org/10.21012/FC12.1145
TT-G:2

INFLUENCE OF PROTECTIVE LAYERS ON THE RESISTANCE OF CONCRETE STRUCTURES UNDER BLAST AND IMPACT LOADING

ALŽBĚTA MĚRKOVÁ[*,1], PŘEMYSL KHEML[*,2], PETR HÁLA[*,3], RADOSLAV SOVJÁK[*,4], LENA LEICHT[†,5], PETR MÁCA[†,6], AND BIRGIT BECKMANN[†,7]

[*] Czech Technical University in Prague, Experimental Centre
Thákurova 7, 166 29 Prague, Czech Republic, www.cvut.cz
[1]e-mail: alzbeta.merkova@fsv.cvut.cz
[2]e-mail: premysl.kheml@fsv.cvut.cz
[3]e-mail: petr.hala@fsv.cvut.cz
[4]e-mail: radoslav.sovjak@cvut.cz

[†]TUD Dresden University of Technology, Institute of Concrete Structures
01062 Dresden, Germany, tu-dresden.de
[5]e-mail: lena.leicht@tu-dresden.dee
[6]e-mail: petr.maca@tu-dresden.de
[7]e-mail: birgit.beckmann@tu-dresden.de

Key words: Textile-Reinforced Concrete, High-Performance Fibre-Reinforced Concrete, Protective Layers, Impact, Blast

Abstract. The rising threat of blast and impact events to critical infrastructure has underscored the need for advanced protective solutions to enhance the durability of structural materials. Protective layers can decrease the damage and increase the resistance of structures against such short-term dynamic loading. Different approaches are presented: dispersed fibre reinforcement and endless-fibre textile reinforcement. High-performance concrete with dispersed fibre reinforcement (HPFRC) is recognised for its exceptional strength and resistance to dynamic loading. However, its performance under blast conditions can be further improved with the addition of protective layers. This study investigates how different protective layers and their position affect the damage and structural behaviour of HPFRC subjected to blast loading. One of the protective layers is pliable and made of polyurethane, the other is stiff and made of glass/epoxy. Experiments were conducted using an explosive, placed in direct contact with the panels, to assess damage under different protective configurations. These configurations included uncoated panels, panels with one-sided stiff coatings, two-sided pliable coatings, and panels with stiff layer on one side and pliable layer on the other. On the other hand, textile-reinforced concrete (TRC) with endless carbon fibre reinforcement is used to strengthen existing structures. On the rear side of an impact-subjected structure, the textile-reinforced strengthening layer enables a membrane action and self-centering effect, reduces scabbing, and increases the perforation limit. On the impact-facing side, strengthening layers consisting of a cover layer and a damping layer decrease the impact energy induced into the concrete structure. The findings of all approaches shown in the work demonstrate the potential benefits of adding protective layers, particularly in reducing the scabbing, while also indicating that certain configurations can reduce the likelihood of full perforation. The results also reveal potential disadvantages of applying protective layers, such as increased cracking and reduced residual capacity of concrete structures.

1 INTRODUCTION

The increasing frequency of extreme loading events, such as blasts and high-velocity impacts, poses significant threats to critical infrastructure, including buildings, bridges, and power plants. Such extraordinary loads often impart high-intensity forces over very short durations, typically lasting only a few milliseconds, leading to catastrophic damage to unprotected structures. The inherent brittleness of concrete makes it particularly vulnerable to spalling, scabbing, and perforation under these conditions. As a result, enhancing the resistance of concrete structures to dynamic loading has become an urgent research priority.

In the context of high-velocity impacts, protective layers have proven effective in enhancing structural performance. Textile-reinforced concrete (TRC) with carbon fibre reinforcement, for instance, enables membrane action and self-centering effects on the rear side of the structure, reducing scabbing and perforation [1].

Protective layers on the impact-facing side have emerged as a promising solution to mitigate damage caused by blast [2] and impact events [3, 4]. These layers developed as hybrid double-layers consist of two sub-layers with different mechanical behavior and different intended functions: damping and cover layers. Damping layers, typically composed of brittle materials with low strength and modulus of elasticity, absorb energy through mechanisms such as elastic deformation, crushing, and densification. Examples include waste tire rubber concrete (WTRC) and lightweight aggregate concrete (LWA). Additionally, pliable coatings, such as polyurea, have been shown to dissipate energy through large deformations, strength, and strain to failure rates of up to 100%, as stated in [5]. Pliable coatings help reduce scabbing and fragment ejection in blast scenarios.

The effectiveness of pliable coatings in improving ballistic protection has been extensively studied across a range of materials, including metal, concrete, and ceramics (e.g., [6–8]), in all cases yielding notable improvements. Recent research has focused on enhancing the ballistic resistance of HPFRC panels by applying pliable coatings. Studies such as [9, 10] demonstrated that HPFRC panels with pliable coatings exhibit significantly higher resistance to ballistic impacts than uncoated panels.

In contrast, cover layers or stiff coatings distribute impact forces over a wider area, enhancing the efficiency of the underlying damping layers. They are made from materials with high strength and modulus, such as fine-grain concrete with embedded textiles (TRC), Strain-Hardening Cementitious Limestone Calcined Clay Composite ($SHLC^3$). According to EHSANI [11], stiff coatings can be applied to structures made of materials such as concrete or masonry with relative ease, using epoxy as an adhesive.

However, the application of protective layers is not without challenges. Certain configurations can lead to increased cracking or reduced residual capacity of the protected structure, necessitating a careful balance between protection and overall performance. This study aims to address these challenges by investigating various protective configurations for RC structures under blast and impact loading. Experimental campaigns assess the behavior of high-performance fibre-reinforced concrete (HPFRC) panels with pliable and stiff coatings, as well as the combination of cover and damping layers. The findings provide valuable insights into the effectiveness of different protective strategies, enabling optimized designs for mitigating extreme loading events.

This paper contributes to the field by presenting a comprehensive analysis of the influence of protective layers on the resistance of RC structures under blast and impact conditions. By combining experimental evidence and theoretical insights, it highlights the potential and limitations of these strategies, paving the way for safer, more resilient infrastructure.

2 MATERIALS AND METHODS

2.1 Strengthening against localized impact loading

At TUD Dresden University of Technology, the damage behaviour of concrete cuboid specimens with two cover layers and two damping layers was studied using a drop tower under hard, localized impact.

The damping layer materials used in this study were prepared based on established mixture designs. (i) The Waste Tire Rubber Concrete (WTRC) mixture was a modified version of the composition proposed by NAJIM AND HALL [12], with 15 wt-% of the natural aggregates replaced by rubber aggregates sized 1 mm to 4 mm, derived from recycled truck tires supplied by [13]. (ii) An Infra-Lightweight Concrete (ILC) mixture, developed by FRENZEL [14], was employed with a higher cement content than in the original design.

Building on the discussion of damping layer materials, this paragraph outlines the details of the cover layer materials used in the specimens. The fine-grain concrete Pagel TF10 CARBOrefit® (P), specifically designed for textile-reinforced concrete, was employed as a matrix material with a maximum grain size of 1 mm. The material properties cited here are based on the work of HERING [15]. For reinforcement of the P cover layer, two layers of carbon textile reinforcement SITgrid 040 KI® were used, oriented at 90° to one another.

The Strain-Hardening Limestone Calcine Clay Composite (SHLC^3) of BEIGH ET AL. [16] represents an advanced form of Strain-Hardening Cementitious Composite (SHCC). To enhance sustainability, limestone and calcined clay partially replaced cement in the matrix. Additionally, 2 vol-% ultra-high-molecular-weight polyethylene (UHMWPE) fibres, 6 mm in length, were incorporated to ensure the strain-hardening effect. For certain SHLC^3 cover layers, reinforcement was further enhanced with two types of 3D hybrid pyramidal truss structures. These structures, combining carbon rovings and high-ductility steel wires, were developed by VO ET AL. [17].

The basic mechanical properties of the C35/45 base cuboids and the materials used for the damping and cover layers are summarized in Table 1.

2.2 Strengthening against blast

At the Czech Technical University in Prague (CTU), the behavior of thin panels made of High-Performance Fibre-Reinforced Concrete (HPFRC) with various coatings was studied under blast loading conditions. The HPFRC was provided as a pre-mixed dry blend, manufactured under controlled industrial conditions to ensure consistent quality. Details regarding the formulation, mixing procedure, and development of the mixture can be found in [18].

To produce the HPFRC samples, the dry blend was mixed with water and fibres (1.5 vol-%) with a total mixing duration of 20 minutes. The mechanical properties of the HPFRC were evaluated using two types of specimens: cylindrical specimens (150 mm in diameter and 300 mm in height) for compressive strength tests, and dog bone specimens (200 mm in length with a reduced cross-sectional area of 50 mm by 100 mm at the center) for tensile strength tests. The results of these tests are summarized in Table 1.

At CTU, two types of protective layers were examined. The first was a pliable layer, created by thoroughly homogenizing a telechelic polyol thinned with castor oil and curing it with an aromatic isocyanate, using a spatula. The second was a stiff layer, produced by combining AEROGLASS® 280 fabric with CHS-EPOXY® 582 resin with TELALIT® 0542 hardener.

2.3 Impact testing procedure and instrumentation

The experimental campaign at TUD was conducted in the drop tower facility of the Otto-Mohr Laboratory (OML, TUD). Detailed descriptions of the experimental methodology and results can be found in LEICHT [4].

An accelerated rigid steel impactor, weigh-

Table 1: Material properties of the base materials: C35/45, and HPFRC with 1.5% fibre volume content (blast tests); damping layer materials; strengthening layer materials.

	Compressive strength (MPa)	**Tensile strength** (MPa)	**Density** (kg/m³)	**Modulus of elasticity** (MPa)
C35/45	50.5	2.7	2256	32,250
HPFRC	90.33	4.2	2351	49,260
WTRC	19.0	2.5	2043	17,694
ILC	10.7	0.3	1128	6516
P	94.3	2.6	2150	32,750
SHLC[3]	71.4	4.4	1963	23,257

ing 21.66 kg with a flat nose, impacted fully-supported RC cuboids strengthened with various material combinations. The impactor, measuring 380 mm in length and 100 mm in diameter, was accelerated to velocities ranging from 20 m/s to 60 m/s. The experiments aimed to identify the most effective material combination for strengthening layers against localized hard impact loading. Three sets of experiments were performed:

1) Reference tests: Experiments on unstrengthened RC cuboids as a baseline.

2) Damping layer variation: Testing different damping layer materials with a consistent cover layer of carbon-fibre-reinforced concrete.

3) Cover layer variation: Evaluating the best-performing damping layer in combination with various cover layer materials.

Figure 1 illustrates the instrumentation of the RC cuboids during the experiments. A Laser Doppler Vibrometer (LDV) was used to record vertical deformations. Three accelerometers (ACC1–3) measured the lateral acceleration, velocity, and deformation at the midpoint of the cuboids' side faces, while ACC4 captured the same parameters in the vertical direction on the top surface of the RC cuboids.

All signals were sampled at a frequency of 200 kHz. Additionally, two high-speed cameras (HSC) recorded the impact at 10,000 fps. These high-speed images facilitated Digital Image Correlation (DIC) analysis, which was used to track the rigid body motion, velocity, and acceleration of both the impactor and the RC cuboids.

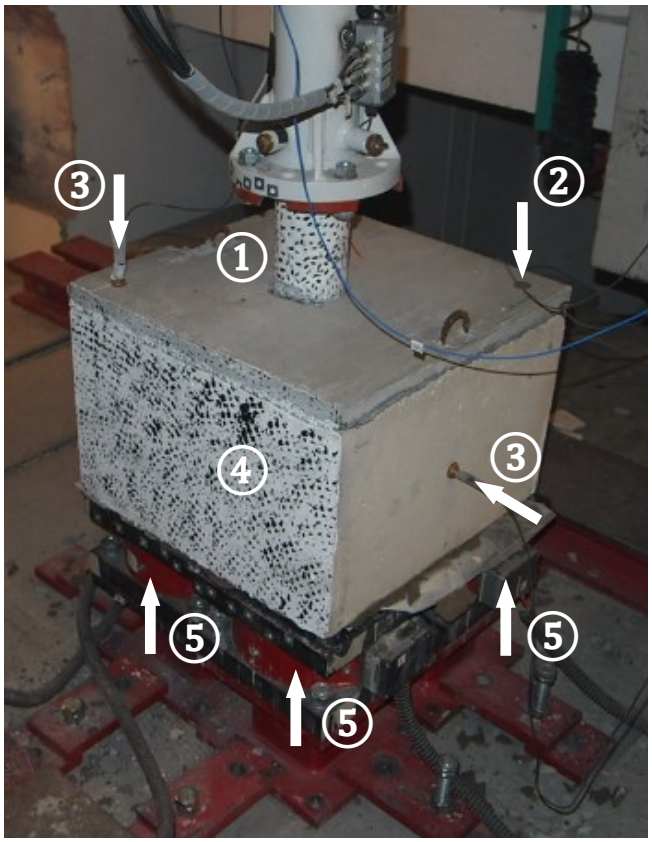

Figure 1: Instrumentation of the RC cuboids: (1) scatter pattern on impactor surface: displacements, velocity, acceleration; (2) Laser Doppler Vibrometer (LDV): displacements; (3) accelerometers (ACC1-4): accelerations; (4) scatter pattern on cuboid surface: displacements, velocity, acceleration; (5) load cells (LC1-4): support forces. From [19].

2.4 Blast testing and instrumentation

Five different protective configurations were considered, including uncoated HPFRC panels, panels with one-sided 4 mm stiff coatings, two-sided 10 mm pliable coatings, panels with 4 mm stiff layer on the front side and 4 mm pliable layer on the back, and panels with 4 mm pliable

layer on the front side and 4 mm stiff layer on the back. The thickness of the HPFRC panel was always 40 mm.

The blast test setup consisted of two steel support structures positioned 800 mm apart, with the tested panel placed horizontally on top, see Fig. 2. A metal detonator with Semtex 1A plastic explosive was centrally placed directly on the top surface of the specimen. The details of the blast tests, including the charge weights and panel configurations, are summarized in Tab. 2. After the blast tests, a detailed scan of the craters in the HPFRC panels was done with the DAVID SLS-2 scanning device.

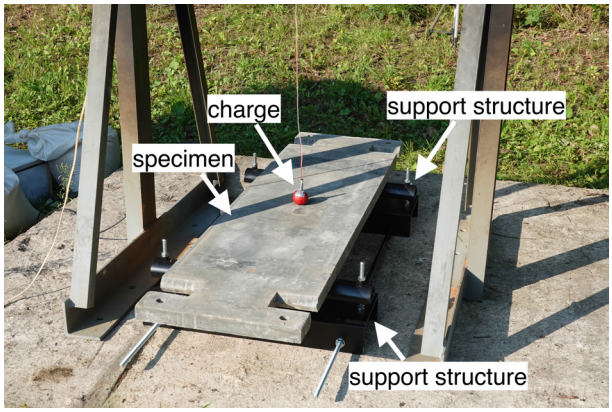

Figure 2: Blast test setup.

3 RESULTS

3.1 Localized impact results

To evaluate the effectiveness of various strengthening layers, force equilibrium analysis was conducted for each specimen. The forces acting on both the impactor and cuboid were calculated by multiplying their respective masses with rigid body accelerations obtained through Digital Image Correlation (DIC). While the rigid body assumption is not fully applicable due to severe damage experienced by unstrengthened cuboids, and DIC measurements were limited to the specimens' front surface, the initial impact response clearly demonstrates that the impactor force is entirely counteracted by the cuboid's inertia. The support force, measured by load cells beneath the specimen, can also be derived from the impactor and cuboid forces [20]. By comparing the calculated and measured support force, we can prove that the rigid body assumption holds for this type of experiment. Post-experimental analysis involved cutting the specimens in halves to evaluate their internal damage.

Analysis of Figures 3 to 6, reveals that the strengthening layers effectively extend the loading impulse duration while reducing peak force magnitude. This modification enables greater impulse transfer to the supports without inducing severe cuboid damage. Figure 3 shows the reference specimen, i.e., the unstrengthened RC cuboid. To show the effect of the hybrid strengthening consisting of the combination of a cover sub-layer and a damping sub-layer, Figs. 4 to 6 show different strengthening configurations. Fig. 4 and Fig. 5 show a strengthening layer consisting of the same cover layer (20 mm of Pagel concrete) and variing damping layers (20 mm of WTRC in Fig. 4 and 40 mm ILC in Fig. 5). Figures 5 and 6 show the same damping layer (40 mm of ILC) and varying cover layers (20 mm of Pagel in Fig. 5, 10 mm of SHCC^3 in Fig. 6).

A notable comparison between force-time profiles in Figures 3 and 5 demonstrates that despite a 10 m/s higher loading velocity, the maximum impactor force decreased. Conversely, the increased support force indicates enhanced force transfer capacity and minimal damage to the cuboid, as can be seen in the saw cuts in Fig. 5. The unstrengthened specimen, Fig. 3, exhibited complete fragmentation even at the lower velocity of 44 m/s. A distinct internal punching cone formation was observed.

The effect of the 20 mm WTRC damping layer combined with a P 20 mm cover layer (Fig. 4) significantly reduced the minimum cuboid force from -2111 kN to -1215 kN compared to unstrengthened RC cuboids (Fig. 3). However, the damping performance of WTRC proved less effective than that of ILC (Figs. 5 and 6) as is evident from the saw cuts. The RC cuboid strengthened with a 20 mm WTRC damping layer and 20 mm P cover layer (Fig. 4)

Table 2: Details of the conducted blast tests, the tested configurations, and blast damage assessment.

Test	Explosive	Layer thickness in mm (with sustained damage after blast tests)				
	weight (g)	Front pliable	Front stiff	HPFRC	Rear stiff	Rear pliable
C1	75	0 (-)	0 (-)	40 (FP)	0 (-)	0 (-)
C2	75	10 (FP)	0 (-)	40 (ED)	0 (-)	10 (SD)
C3	75	0 (-)	0 (-)	40 (FP)	4 (ND)	0 (-)
C4	150	0 (-)	0 (-)	40 (FP)	4 (SD)	0 (-)
C5	150	4 (CD)	0 (-)	40 (CD)	4 (SD)	0 (-)
C6	150	0 (-)	4 (FP)	40 (FP)	0 (-)	4 (FP)

demonstrated visible but notably reduced damage compared to the unstrengthened specimen (Fig. 3). The cracking pattern suggests that while WTRC did not provide complete protection, it effectively mitigated damage to the cuboid.

Saw cuts of the specimens utilizing the 40 mm ILC damping layer, combined with either the 20 mm P (Fig. 5) or 10 mm SHLC[3] (Fig. 6) cover layer reveal that the cuboids maintained complete internal structural integrity despite being subjected to higher impactor velocities.

3.2 Blast response

Experimental investigations conducted at CTU in Prague aimed to evaluate the effectiveness of various protective coatings and their configurations in mitigating damage to HPFRC panels subjected to direct contact blast loading. Table 2 summarizes the damage sustained by the HPFRC panels and the additional protective layers across all configurations. The following nomenclature is used in the table: ND (no damage), SD (surface damage), ED (extensive damage without full perforation), FP (full perforation), and CD (complete damage with no residual strength).

As shown in Table 2, all HPFRC panels were perforated except C2, which had pliable layers on both sides. C5, with a pliable front and stiff rear layer, underwent complete perforation and collapse, losing all residual strength.

A bare HPFRC panel was tested as a reference, with results for the impact and rear sides shown in Fig. 7. A clean crater formed with few longitudinal cracks on both sides and one diagonal crack on the rear extending to the edge.

Fig. 8 shows the impact of a 75 g direct contact blast on the charge-facing side of the HPFRC panel in C2 with pliable protective layers on the front and rear sides. Compared to bare panels, more cracks appeared on both sides, with circumferential tendencies on the impacted face. The protective layers prevented perforation but caused greater edge damage and fragmentation, likely due to the pliable rear layer reflecting part of the blast wave, increasing energy absorption by the panel.

Fig. 9 shows the damage from a 75 g charge on the impact-facing (a) and rear (b) sides of the HPFRC panel in C3. Similarly, Figure 10 illustrates the effects of a 150 g charge in C4. Both configurations, with stiff rear layers, exhibit front-face cracking similar to bare panels, though the 150 g charge results in more cracks. Notably, C4 shows a transverse crack extending from the crater to both edges, with relatively clean craters in both setups.

Fig. 11 depicts the damage to the HPFRC panel in C5 (pliable front layer, stiff rear layer) under a 150 g charge. The panel was completely destroyed, losing all residual strength. The front side shows a highly fragmented crater with edge damage, though fewer cracks compared to C2, with similar circular patterns. The rear side exhibits a few radial cracks extending from the crater to the edges.

Fig. 12 shows the damage to the HPFRC panel in C6 under a 150 g charge. Each side features a transverse crack from the crater to the edges, while the front-side crater is clean, similar to the bare panel and C3 and C4. Only a few longitudinal cracks are visible on both sides.

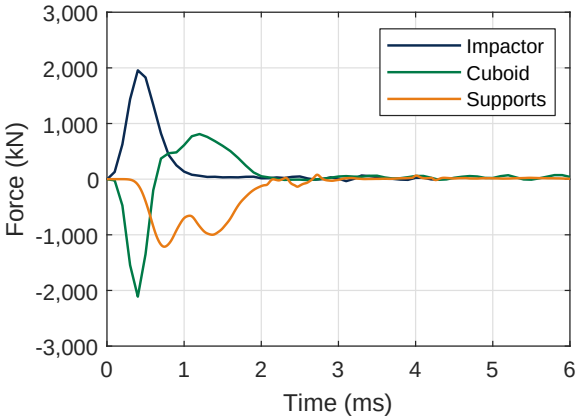

Figure 3: Force equilibrium and saw cut of an unstrengthened RC cuboid. Impactor velocity: 44 m/s.

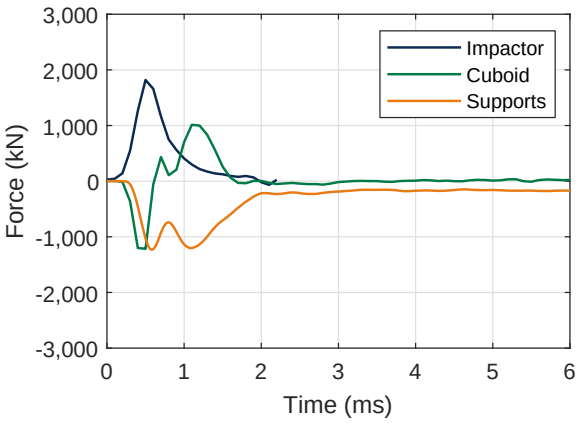

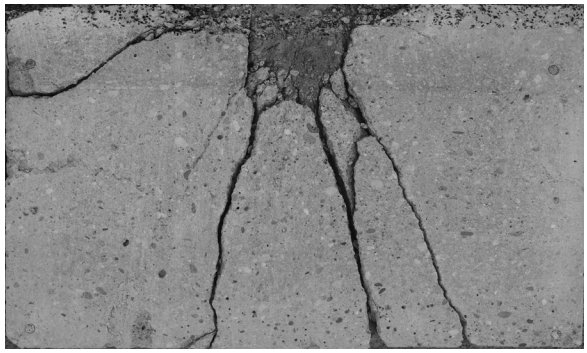

Figure 4: RC cuboid with WTRC 20 mm damping layer and Pagel (P) 20 mm cover layer. Imp. vel.: 44 m/s.

The crater areas on both surfaces of all panels were scanned and summarized in Table 3. The bare panel showed the smallest front crater area, followed closely by C3 with only a stiff rear layer, highlighting that the absence of a front coating allowed the blast wave to propagate through the panel. C3 also had a smaller back crater than the bare panel, demonstrating the stiff rear layer's positive impact.

Adding a front pliable layer to the HPFRC core with a rear stiff layer negatively impacted the craters formed on both sides of the panel. While being subjected to the same charge weight, in C4, the front crater area increased by 25% and the back crater area increased by 38%, compared to C3. C2, with both pliable coatings, showed the largest crater areas under a 75 g charge, while C6, with a stiff front layer, reduced the back crater area despite a 150 g charge.

Table 3: The area of craters obtained by scanning.

Test	Front surface crater (mm^2)	Back surface crater (mm^2)
C1	3 005.63	21 196.55
C2	4 253.87	26 817.22
C3	3 461.83	16 337.38
C4	6 435.11	23 908.17
C5	8 030.02	33 093.48
C6	7 200.95	25 840.11

Scabbing occurred on the rear face of HPFRC panels in all tests where it was unreinforced or the rear layer detached during the blast. Stiff rear layers failed to prevent scabbing when detached. In C2 (pliable rear layer, 75 g charge), all fragments were contained as the layer adhered without rupturing. In C6 (150 g charge), scabbing was partially mitigated; the pliable rear layer adhered but was breached by the blast.

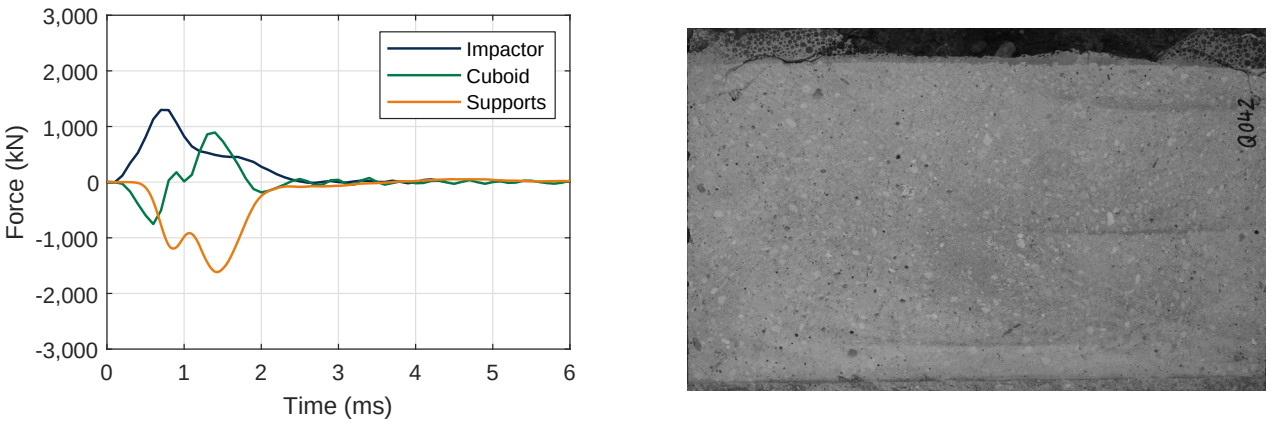

Figure 5: ILC 40 mm damping layer, P 20 mm cover layer. Impactor velocity: 54 m/s.

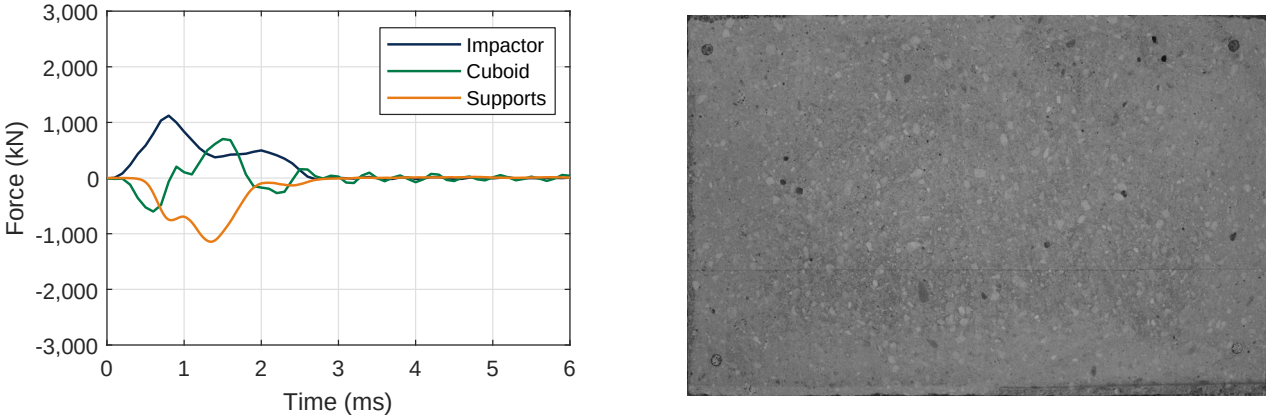

Figure 6: ILC 40 mm damping layer, SHLC^3 10 mm cover layer. Impactor velocity: 54 m/s.

4 DISCUSSION

4.1 Localised impact

The results of the hard impact on concrete cuboids protected by strengthening layers demonstrate that the 40 mm ILC damping layer provided sufficient energy absorption capacity in combination with a cover layer to ensure comprehensive protection of the RC specimens against impact forces. The minimal cuboid inertial force was -2111 kN for the unstrengthened specimens, compared to -1215 kN for the WTRC specimens, -419 kN for the ILC specimens with a P cover layer, and -448 kN for the ILC specimens with an SHLC^3 cover layer.

A comparative analysis of the P and SHLC^3 cover layers at identical impactor velocities (Figs. 5 and 6) reveals negligible differences in the force-time profiles and the aforementioned minimal force values. However, the fibre reinforcement in the SHLC^3 cover layer exhibited superior resistance to front-face spalling, making this cover layer the preferred choice.

4.2 Blast

Exposing a bare HPFRC panel (C1) to a 75 g Semtex 1A blast caused complete perforation, as in [21]. Pliable layers in C2 prevented perforation, while the rear stiff coating in C3 did not. C3 exhibited scabbing, but with a smaller back surface crater than the bare panel. The rear stiff layer in C3 detached, while C2's pliable layer adhered, containing all fragments. C2 showed a 25% increase in crater areas due to partial blast wave reflection, consistent with [22].

Under a 150 g charge, C5 (front pliable, rear stiff) sustained the most damage, with crater areas 25% and 40% larger on the front and back than C4, and over 10% and 30% larger than C6. In contrast, C4 (rear stiff only) exhibited the smallest craters, reducing back crater area by

(a) blast side (b) rear side

Figure 7: Bare HPFRC panel subjected to a 75 g charge direct contact blast. C1.

(a) blast side (b) rear side

Figure 8: HPFRC panel with front and rear pliable layers subjected to a 75 g charge direct contact blast. C2.

30% compared to the bare panel. However, C4 had deeper transverse cracks, indicating lower residual strength.

Scabbing occurred in all 150 g tests, but C6 partially mitigated rear fragments with its pliable rear layer. C2 and C5 showed circumferential cracking, similar to 'hoop cracks' observed by HOU ET AL. [23] in polyurea-coated steel plates under air blasts, due to deformation differences between the panel and coating.

5 CONCLUSIONS

This study compares protective layer designs from TUD and CTU, investigating strategies to enhance reinforced concrete resistance to localized impact and blast loads. Through experimental research, we explored damping and protective layers, including pliable and stiff coatings.

At TUD, the experiments focused on damping layers made from WTRC and ILC, combined with cover layers P and SHLC[3]. Key find-

(a) blast side (b) rear side

Figure 9: HPFRC panel with a stiff rear layer subjected to a 75 g charge direct contact blast. C3.

(a) blast side (b) rear side

Figure 10: HPFRC panel with a stiff rear layer subjected to a 150 g charge direct contact blast. C4.

(a) blast side (b) rear side

Figure 11: HPFRC panel with a pliable front and stiff rear layer subjected to a 150 g charge direct contact blast. C5.

ings from the hard impact tests include:

1) The 40 mm ILC layer showed superior damping performance due to efficient energy absorption through densification.

2) The 10 mm SHLC[3] layer was the optimal cover, enhancing load distribution and crack control, enabling optimal ILC activation.

3) The ILC-based protective system successfully prevented RC cuboid damage at impactor velocities up to 55 m/s (200 km/h). The damping layer material had a greater impact on overall performance than the cover layer.

4) The cuboid experimental setup proved efficient for evaluating strengthening layer performance, offering a practical methodology for future investigations.

At CTU, the focus was on HPFRC panels under direct-contact explosions. Two protective layers (pliable and stiff) were tested in different configurations. Blast results revealed:

1) Pliable coatings on both sides prevented perforation under a 75 g charge but caused larger craters due to blast wave reflection and increased energy absorption.

(a) blast side (b) rear side

Figure 12: HPFRC panel with a stiff front and pliable rear layer subjected to a 150 g charge direct contact blast. C6.

2) Panels with only rear stiff coatings showed reduced back surface craters but failed to prevent perforation or contain fragments.

3) A front pliable and rear stiff configuration suffered the greatest damage under a 150 g charge, with the largest craters and no residual strength.

4) A rear stiff layer under a 150 g charge had smaller craters than a front stiff and rear pliable layer, but deeper cracking, indicating reduced residual strength.

5) Panels with front pliable layers showed extensive cracking and circumferential 'hoop cracks' due to deformation mismatches.

These findings demonstrate the potential of tailored protective coatings for mitigating damage and improving structural integrity under extreme conditions. Future research should focus on the long-term durability, behavior under repeated loading, and scalability for real-world applications, advancing safety and resilience in critical infrastructure.

ACKNOWLEDGEMETNS

This publication was supported by the Czech Science foundation [23-06352S1] and the Grant Agency of the CTU in Prague [OHK1-021/25] as well as the German Research Foundation (Deutsche Forschungsgemeinschaft, DFG) in the framework of Research Training Group (Graduiertenkolleg, GRK) 2250, entitled "Mineral-bonded composites for enhanced structural impact safety" (grant nr. 287321140), and by Federal Ministry for the Environment, Nature Conservation, Nuclear Safety and Consumer Protection based on a decision by the German Bundestag under project No. 1501647.

REFERENCES

[1] Bracklow, F., Jackson, C.M., Signorini, C., Jacques, E., Beckmann, B., Curbach, M., and Mechtcherine, V. 2025. Hybrid mineral-bonded protective layers for enhanced self-centering capacity of reinforced concrete beams subjected to blast. *Engineering Structures* **322**:119151.

[2] Leicht, L., Colombo, M., Martinelli, P., Signorini, C., Mechtcherine, V., di Prisco, M., Scheerer, S., Curbach, M., and Beckmann, B. 2025. Protective potential of high-contrast mineral-bonded layers on reinforced concrete slabs subjected to uniform shock waves. *International Journal of Impact Engineering* **196**:105149.

[3] Leicht, L., and Beckmann, B. 2024. Development of strengthening layers against localized impact loading. In Mechtcherine, V., Signorini, C., and Junger, D. (eds), *Transforming Construction: Advances in fibre Reinforced Concrete (Proceedings of XI RILEM-fib International Symposium on fibre Reinforced Concrete)*.

[4] Leicht, L. 2024. Characterization of mineral-bonded composites as damping layers against impact loading. Dissertation, Technische Universität Dresden.

[5] Chundawat, T. S., Vaya, D., Sini, N. K., Varma, I.K. 2016. Blast Mitigation Using FRP Retrofitting and Coating Techniques. *Polymer Composites* **39(5)**:1389-1402.

[6] Si, P., Liu, Y., Yan, J., Bai, F., Shi, Z., and Huang, F. 2023. Effect of polyurea layer on ballistic behavior of ceramic/metal armor. *Structures* **48(6910)**:1856-1867.

[7] Liu, Q., Guo, B., Chen, P., Su, J., Arab, A., Ding, G., Yan, G., Jiang, H., and Guo, F. 2021. Investigating ballistic resistance of CFRP/polyurea composite plates subjected to ballistic impact. *Thin-Walled Structures* **166**, Article 108111.

[8] Zhang, P., Wang, Z., Zhao, P., Zhang, L., Jin, X. C., and Xu, Y. 2019. Experimental investigation on ballistic resistance of polyurea coated steel plates subjected to fragment impact. *Thin-Walled Structures* **144**, Article 106342.

[9] Hála, P., Perrot, A., Vacková, B., Kheml, P., and Sovják, R. 2023. Experimental

and numerical study on ballistic resistance of polyurethane-coated thin HPFRC plate. *Materials Today: Proceedings* **93**:607-613.

[10] Hála, P., Kheml, P., Perrot, A., Mašek, J., and Sovják, R. 2023. Lightweight Protective Sandwich Structure with UHPC Core. *International Interactive Symposium on Ultra-High Performance Concrete* **3(1)**, Article 16.

[11] Ehsani, M. and Peña, C. 2009. Blast Loading Retrofit of Unreinforced Masonry Walls with Carbon fibre Reinforced Polymer (CFRP) Fabrics. *Structure Magazine* **20**.

[12] Najim, K.B., and Hall, M.R. 2012. Mechanical and dynamic properties of self-compacting crumb rubber modified concrete. *Construction and Building Materials* **27**(1): 521–530.

[13] Mülsener Rohstoff- und Handelsgesellschaft mbH. 2024. Gummigranulat W 1040. https://mrh-muelsen.com/produktspezifikation-gummigranulat-w-1040.html. *Beton- und Stahlbetonbau* **107**: 15–22.

[14] Frenzel, M., and Curbach, M. 2018. Shear strength of concrete interfaces with infralightweight and foam concrete. *Structural Concrete* **19**(1): 269–283.

[15] Hering, M. 2020. Untersuchung von mineralisch gebundenen Verstärkungsschichten für Stahlbetonplatten gegen Impaktbeanspruchungen. Dissertation, Technische Universität Dresden.

[16] Beigh, M.A.B., Signorini, C., and Mechtcherine, V. 2022. Rheological characterization of the strain hardening limestone calcined clay cement (SHLC³) composites for shotcreting [PowerPoint presentation]. Oral Presentation at the 4th International Conference on Calcined Clays for Sustainable Concrete, Lausanne, Switzerland, July.

[17] Vo, D.M.P., Sennewald, C., Golla, A., Vorhof, M., Hoffmann, G., Xuan, H.L., Nocke, A., and Cherif, C. 2022. Textile-based 3D truss reinforcement for cement-based composites subjected to impact loading Part I: Development of reinforcing structure and composite characterization. *Materials Science Forum* **1063**: 121–132.

[18] Bažantová, Z. et al. 2016. Multi-Functional High-performance Cement Based Composite. *Key Engineering Materials* **677**:53–56. **17**:306-316.

[19] Leicht, L. 2022. Charakterisierung von mineralisch gebundenen Kompositen zur Impaktdämpfung. In *61. Forschungskolloquium des Deutschen Ausschusses für Stahlbeton (DAfStb)*, Dresden, pp. 25–28. Deutscher Ausschuss für Stahlbeton. [in German]

[20] Máca, P., Leicht, L., Schubert, T., and Beckmann, B. 2024. Experimentelle Untersuchung von Stahlbetonbalken ohne Bügelbewehrung unter Stoßbelastung. *Beton- und Stahlbetonbau*, **119**(4): 272–283. [in German]

[21] Mára, M. et al. 2020. Experimental Investigation of Thin-Walled UHPFRCC Modular Barrier for Blast and Ballistic Protection. *Applied Sciences* **10(23)**:8716.

[22] Amini, M. R., Isaacs, J. B., and Nemat-Nasser, S. 2010. Experimental investigation of response of monolithic and bilayer plates to impulsive loads. *International Journal of Impact Engineering* **37(1)**:82-89.

[23] Hou, H., Chen, C., Cheng, Y., Zhang, P., Tian, X., Liu, T., and Wang, J. 2019. Effect of structural configuration on air blast resistance of polyurea-coated composite steel plates: Experimental studies. *Materials & Design* **182**:108049.